# Supporting Information for

# Confined Molecular Motion across Liquid/liquid Interfaces in a Triphasic Reaction towards Free-standing Conductive Polymer Tube Arrays

Tuo Ji,[a] Wei Cao,[b] Long Chen,[a] Liwen Mu,[a] Huaiyuan Wang,[c] Xiong Gong,[d], Xiaohua Lu[b] and Jiahua Zhu[a*]

[a] Intelligent Composites Laboratory, Department of Chemical and Biomolecular Engineering, The University of Akron, Akron, OH 44325 USA
[b] State Key Laboratory of Material-Oriented Chemical Engineering, College of Chemistry and Chemical Engineering, Nanjing Tech University, Nanjing, 210009, P. R. China.
[c] College of Chemistry and Chemical Engineering, Northeast Petroleum University, Daqing, 163318, P.R. China
[d] Department of Polymer Engineering, The University of Akron, Akron, OH 44325 USA
∗Corresponding author E-mail: jzhu1@uakron.edu

## S1. METHODS

***Materials*:** Aniline (≥99.5%), pyrrole (≥98%), ammonium persulfate (APS ≥98%), perfluorooctanoic acid (PFOA, ≥98%), *p*-Toluenesulfonic acid monohydrate (PTSA ≥98%), methacrylic acid (>99%), chloroform (≥99.5%) and toluene (≥99.5%) were purchased from Sigma Aldrich. Xylenes (≥99.9%), hydrochloride acid (HCl 37.4%) were purchased from Fisher Scientific. N-methylpyrrolidone (NMP ≥99.5%) was purchased from BDH. Oleic acid was purchased from Shanghai Lingfeng Chemical Reagent Co. Ltd. All reagents were used as received. Deionized water was used for all experimental process.

***Synthesis of polyaniline & polypyrrole arrays:*** The experimental setup consists three liquid phases: oxidant (APS) and doping acid (PTSA) in inner aqueous phase, organic monomer (aniline, pyrrole) in outer aqueous phase and these two aqueous phases were separated by an organic solvent phase. The outer aqueous phase with organic phase forms IF1 and inner aqueous phase with organic phase forms IF2, refer to Figure 1. Specifically, aniline (or pyrrole, 0.03~0.1 M) was firstly dissolved in 3.0 mL $H_2O$ and added into a vial with inner diameter (ID) of 23 mm. A given ratio of APS/PTSA was dissolved in 2.0 mL $H_2O$ and added into another smaller vial with ID of 12 mm. The small vial was sit at the central of larger vial and then 14.0 mL organic solvent (toluene, xylene or chloroform) was added slowly to form a steady triphasic system. For comparison, conventional biphasic synthesis was conducted in the small vial.

***Characterization:*** The surface morphology of samples was characterized by scanning electron microscope (SEM, JEOL-7401) with a sputter-coated gold. Samples for transmission electron microscopy (TEM, FEI) analysis were prepared on carbon-coated copper grids and further characterized with an accelerating voltage of 120 kV. The contact angles of distilled water and glycerin were determined by the sessile drop technique on a Rame-Hart contact angle

goniometer. Eight samples were measured in order to obtain the average values of contact angles. The Fourier transform infrared (FT-IR, Digilab Excalibur FTS 3000) spectra were collected by using KBr pressed disks with 1 $cm^{-1}$ resolution. The UV-vis spectra were collected on a Hitachi 4100 UV-vis spectrophotometer. X-ray photoelectron spectroscopy (XPS) was carried out on a PHI VersaProbe II Scanning XPS Microprobe using Al K α line excitation source. The powder X-ray diffraction analysis was carried out with a Bruker AXS D8 Discover diffractometer with GADDS (General Area Detector Diffraction System) operating with a Cu-K α radiation source filtered with a graphite monochromator (λ = 1.541 Å). The conductivity of polyaniline was measured via a three-electrode method on a VersaSTAT 4 electrochemical workstation (Princeton Applied Research). Briefly, the polyaniline samples were pasted on the graphite electrode mixed with Polyvinylidene fluoride and carbon black (80:10:10). Pt wire was used as counter electrode and saturated calomel electrode was used as reference. Electrochemical impedance spectroscopy (EIS) tests were performed by use of a sinusoidal signal with mean voltage of 0 V and amplitude of 10 mV over a frequency range of 1000000-0.01 Hz.

***Molecular dynamics (MD) simulation:*** MD simulation was adopted to investigate the diffusion behavior of aniline at the toluene-water interface. The OPLS−AA force field[17] was used for both toluene and aniline molecules. The water molecule was modeled by single-point charge/extended.[18] The interaction between molecules includes both van der Waals and electrostatic terms. The former one is described by the 12−6 Lennard−Jones potential $U_{LJ} = 4\varepsilon[(\sigma/r)^{12} - (\sigma/r)^{6}]$ as a function of the interatomic distance $r$. The latter one is described by Coulomb's law. To match the experimental setup, oil/water interface was constructed by 4180 water and 710 toluene molecules with 65 aniline molecules randomly scatterred either in toluene or water phase. Simulation was performed with LAMMPS software package.[19] Langevin

dynamics were firstly applied to randomize the initial shape of the molecules to speed up equilibration. Then, simulations were performed in the NPT ensembles at 300 K and 0.1 MPa for 10 ns. The particle-mesh Ewald summation[20] was used for the electrostatic interactions, and a cutoff of 1.0 nm was used for the calculation of van der Waals interactions. Periodic boundary condition was used in all three dimensions. A 1.0 fs time step was used, and output coordinates were obtained every 1.0 ps.

## S2. RESULTS

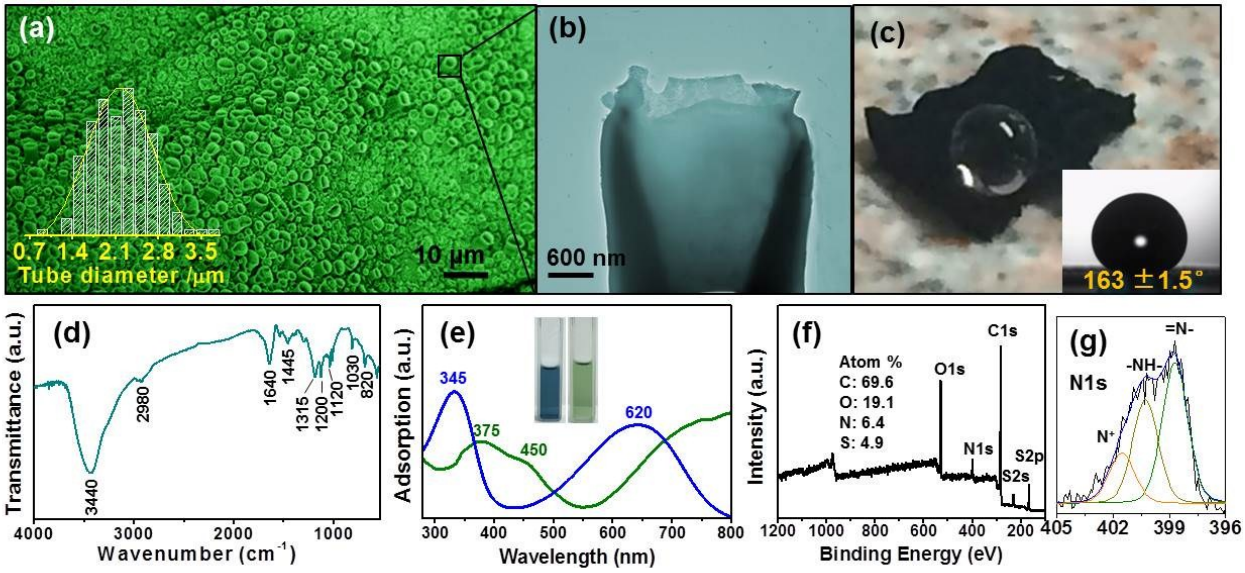


**Figure S1. (**a) SEM image of polyaniline tube array, inset: statistic distribution of tube diameter, (b) TEM image of polyaniline tube array, (c) experimental photo of a water droplet on the doped PANI film, (d) FT-IR spectrum, (e) UV-visible spectra, and (f) overall XPS and (g) N1s deconvolution results. Conditions: aniline/APS/PTSA = 1:0.6:7.3, temperature: 4 $^{o}$C, reaction time: 72 h.

In Figure S1(a), the polyaniline film surface facing the organic phase shows well-patterned tube array structures with diameter of 2.2±0.4 μm, while the surface facing aqueous phase is relatively smooth (Figure S2). The thickness of polyaniline film is about 5.5 μm, Figure S10. The different surface morphologies at both sides reveal the directional growth of the array structure towards the "oil" phase. The tubular morphology is also confirmed by TEM, Figure

S1(b) and S11. It is observed that the interior space of the microtube shows funnel-shaped structure. This unique microscale geometric structure together with the nanoscale surface texture provides a good combination of micro- and nano- hierarchical morphology, which is an essential component for superhydrophobic surfaces. To reduce surface energy, this material is dedoped by ammonia and then redoped by perfluorooctanoic acid. Subsequently, superhydrophobic property is achieved with water contact angle of $163 \pm 1.5^{o}$, Figure S1(c).

The FT-IR spectra in Figure S1(d) with adsorption peaks at 3440 $cm^{-1}$ (N-H stretching), 1640 $cm^{-1}$ (C=C stretching), 1540 and 1445 $cm^{-1}$ (quinoid and benzenoid ring, respectively), 1315 $cm^{-1}$ (C-N stretching) and 820 $cm^{-1}$ (1,4-substituted phenyl ring stretching) are corresponding to the emeraldine form of polyaniline.[14a] The peaks at 1170 and 1050 $cm^{-1}$ can be assigned to the asymmetric and symmetric O=S=O stretching vibrations, respectively, indicating the existence of $SO^{3-}$ groups from doping acid PTSA. The emeraldine base and emeraldine salt forms of PANI are also supported by the UV-Vis spectrum, Figure S1(e). The spectra for the emeraldine base (blue curve) has two adsorption peaks at 345 and 620 nm, ascribing to the $\pi$-$\pi^*$ transition of the benzenoid rings and the exciton absorption of the quinoid rings, respectively.[17] In the doped emeraldine salt (green curve), two adsorption peaks at 375 and 450 nm appeared indicating the protonation of the imine sites.[17-18] The red shift from 345 to 375 nm and the appearance of an upshift at ~800 nm are related to a doping level and the formation of a polaron band transition.[19] By confirming the doping state of PANI, XPS is then used to quantify the surface elemental composition and chemical bonding of the polyaniline tube array, Figure S1(f). The full scan spectrum shows five major peaks, C1s (281.7 eV), O1s (529.7 eV), N1s (398.7 eV), S2p (164.7 eV) and S2s (230.3 eV) with elemental composition of C (69.6 at%), O (19.1 at%), N (6.4 at%) and S (4.9 at%), respectively. N1s peak can be further resolved

into three peaks: quinonoid imine (=N- , 398.7 eV), benzenoid amine (-NH-, 400.3 eV), and positively charged nitrogen (N+, 401.5 eV), Figure 3(g). The higher peak intensity of =N- than that of –NH- indicates that more quinoniod imine structure is formed than benzenoid amine. Meanwhile, the doping ratio of PANI calculated by $N^+/N$ ratio is about 0.22, which is in good agreement with other literature reports.[20]

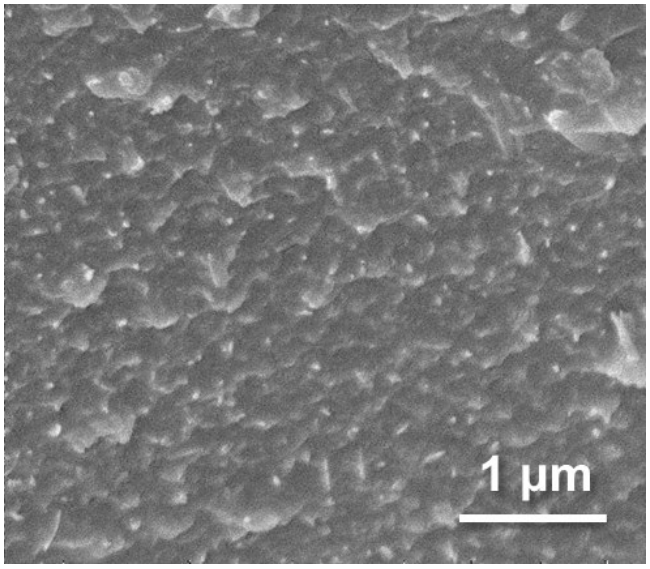


**Figure S2.** The SEM image of the reverse side of PANI film.

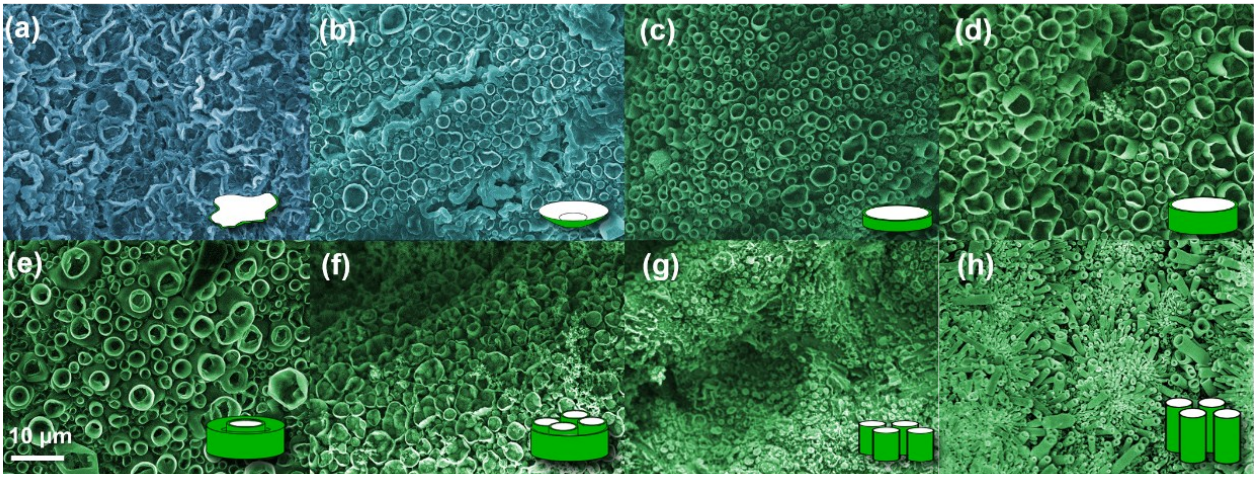


**Figure S3.** Typical SEM images of the PANI tube array synthesized at different polymerization times: (a) 4 h, (b) 8 h, (c) 16 h, (d) 24 h, (e) 32 h (f) 40 h (g) 48 h and (h) 72h; Conditions: aniline/APS/PTSA = 1:0.6:7.3, 4 $^{o}$C.

To understand the tube array structure formation mechanism on the free-standing film, the structure evolution was monitored at different reaction times, Figure S3. Generally, the morphology change can be roughly divided into three stages: mother-tube growth→tube division→daughter-tube growth. At first stage, PANI tubes with diameter of 3~8 μm was formed and grew along the tube axial direction, Figure S3(a-d). At early stage of reaction (<4 h), blue thin film was formed at the interface with wrinkled sheet structure. With reaction proceeds to 8 h, the sheets curled up to form bow-like structures on the PANI film surface. It is also worth mentioning that the PANI film turns into green color after 8 hours, indicating the doped emeraldine salt as evidenced by UV-Vis spectrum, Figure S4. The color change also reveals that PTSA has successfully integrated into the PANI backbone structure and played an important role in PANI morphology control. Further growth of PANI into longer tubes has been observed with reaction proceeds to 24 h, Figure S3(d). The second tube division stage is initiated after 24 h reaction and completed within 40 h, Figure S3(e-g). With further tube growth, the tube wall became thicker and some supportive structure was generated inside the tubes. These interior structures turned into individual compartments and eventually break down the mother-tube structure. At last stage, these compartments served as individual reactive sites to grow smaller daughter-tubes with diameter of 1~2 μm until the reaction was forced to complete at 72 h, Figure S3(h).

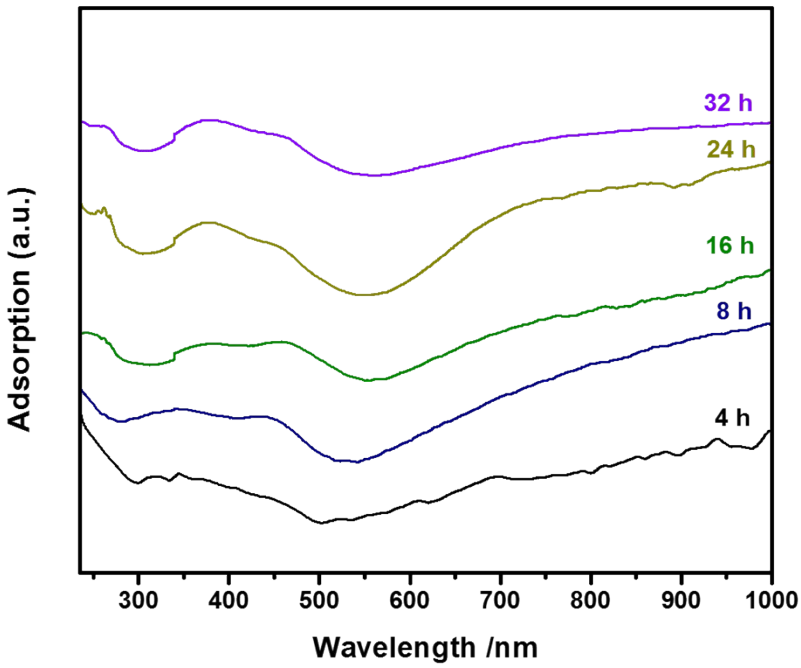


**Figure S4.** UV-Vis spectrum of the PANI tube array synthesized at different polymerization times.

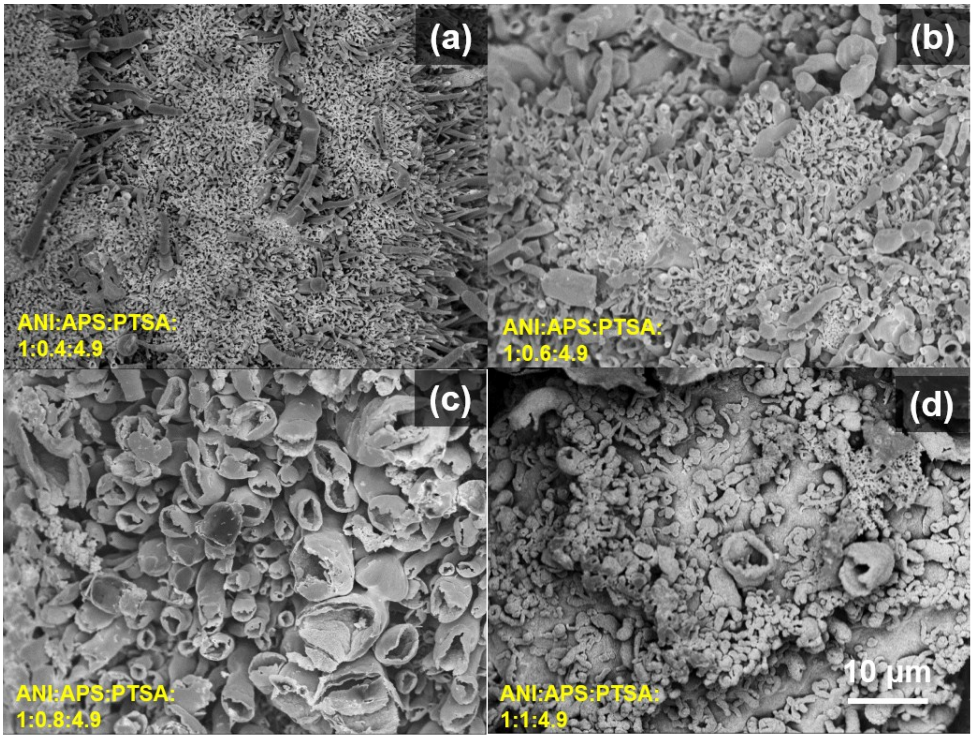


**Figure S5.**The morphology of polyaniline tube array by different concentrations of APS.

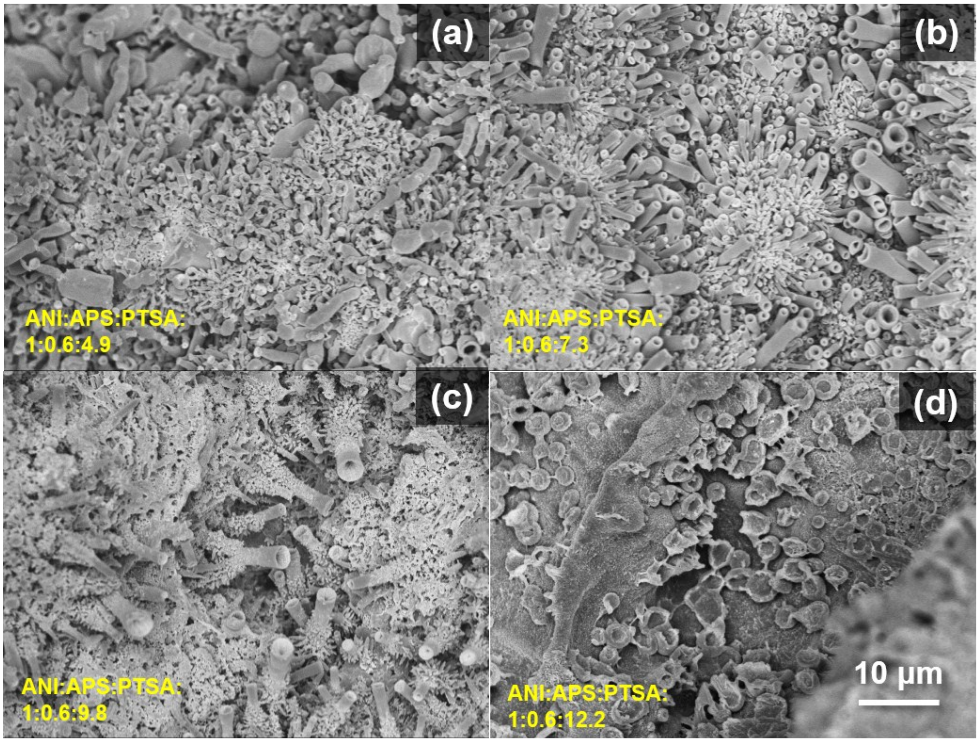


**Figure S6.** The morphology of polyaniline tube array by different concentrations of PTSA.

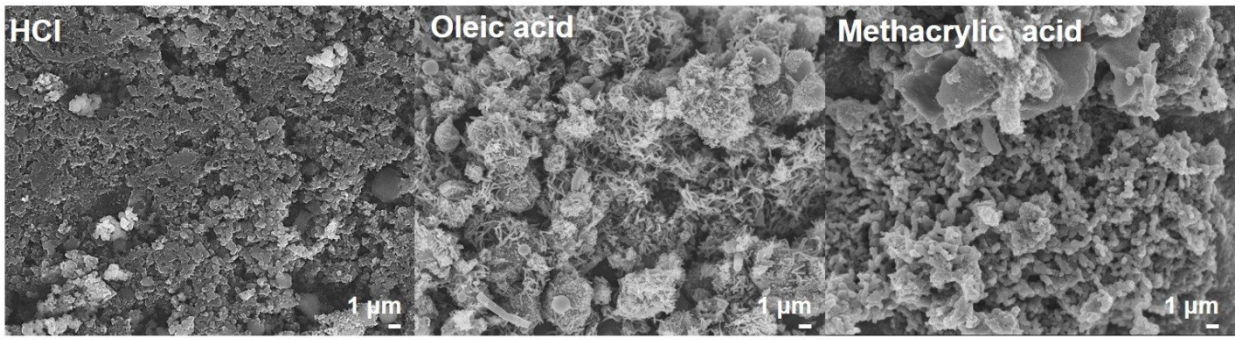


**Figure S7**. SEM images of PANI synthesized by using different doping acids, HCl, Oleic acid and methacrylic acid.

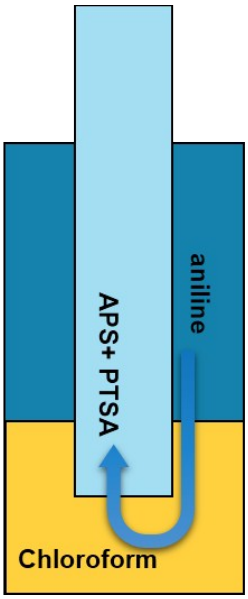


**Figure S8.** The illustration of triphasic method by using chloroform as organic phase.

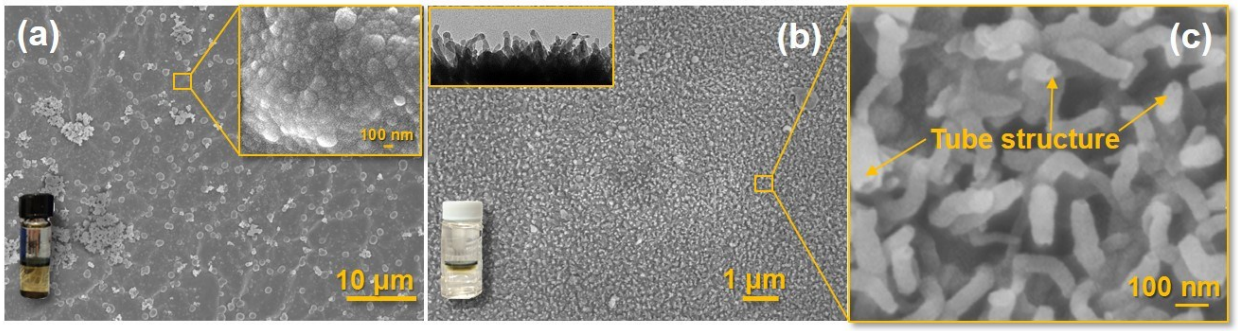


**Figure S9.** SEM morphology of polypyrrole film synthesized by (a) "water/oil", inset image shows enlarged magnification and (b) "water/oil/water" method, inset shows TEM image of vertically patterned nanofiber morphology, (c) enlarged SEM surface morphology of polypyrrole thin film shows nanotube structure.

This "water/oil/water" system has been successfully applied to synthesize other conductive polymer tube arrays such as polypyrrole. In the conventional "water/oil" system, a freestanding thin film was also obtained together with partially precipitated particles at the bottom of the vial, Figure S9(a). Focusing on the thin film surface, aggregated polypyrrole nanoparticles were observed, inset of Figure S9(a). By taking the "water/oil/water" reaction

system, all the polymerized products stay at the interface without any precipitates, inset photo of Figure S9(b). More importantly, densely patterned nanofibrous materials were observed on the thin film surface with vertically arrayed pattern, top inset of Figure S9(b). Clear tube structure was observed in the enlarged SEM image, Figure S9(c), where the tube inner diameter is measured as 18~20 nm, outer diameter of 18-23 nm and tube length of 100~270 nm, Figure S9(c). The different product morphologies from the two synthetic methods are induced by the diffusion control of pyrrole monomer to the reactive interface.

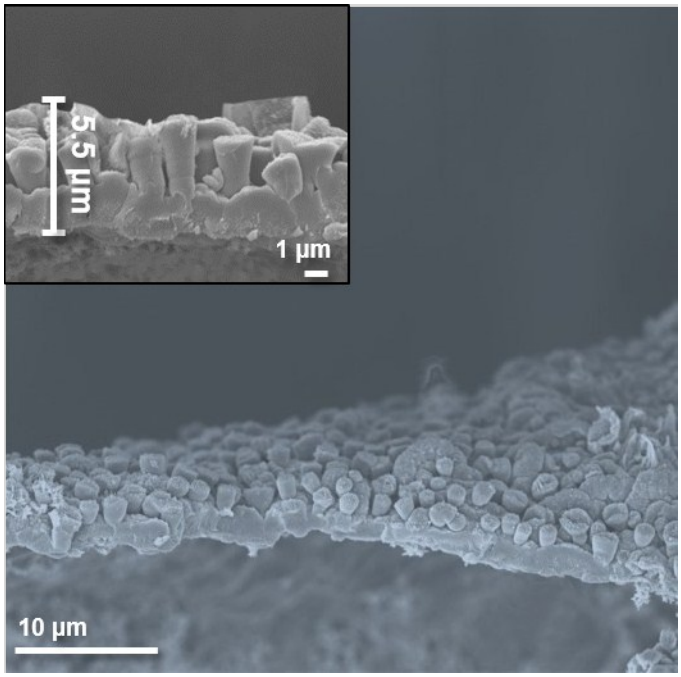


**Figure S10.** SEM image of the cross section of polyaniline film.

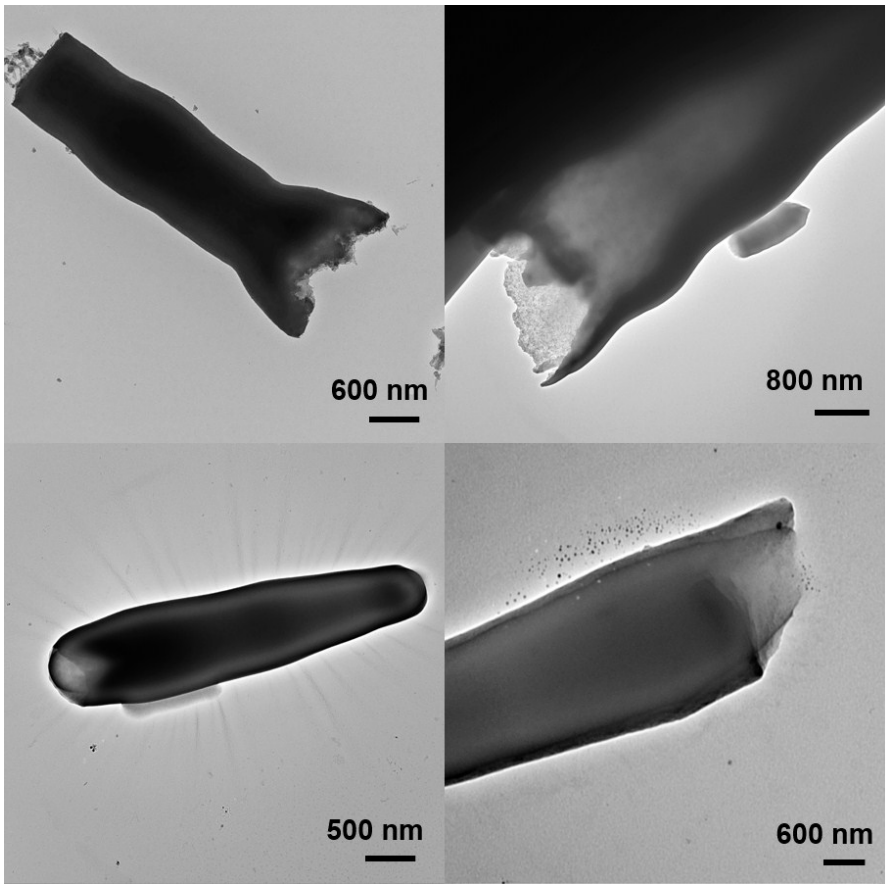


**Figure S11.** TEM images of polyaniline tubes.

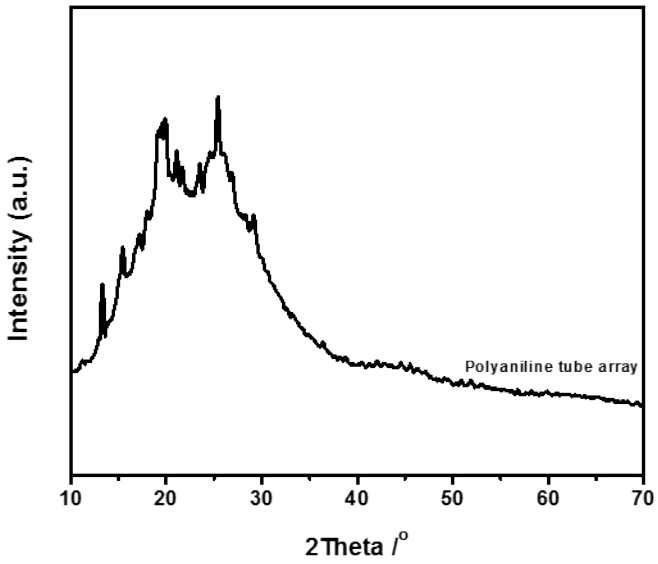


**Figure S12.** X-ray diffraction sprctrum of polyaniline film.

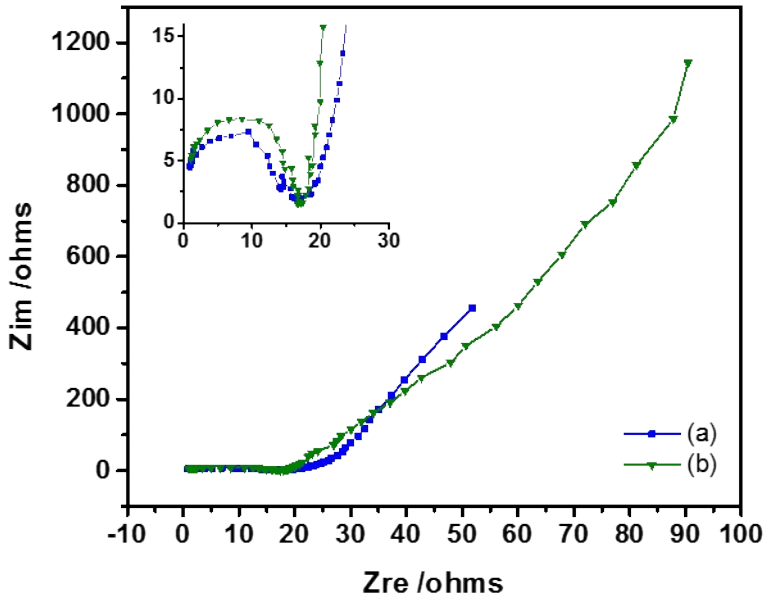


**Figure S13.** Electrochemical impedance spectroscopy test of polyaniline (a) tube array film and (b) tube powder.